h_c Production at Hadron Colliders

Jian-Xiong Wang[2,3] and Hong-Fei Zhang[1,2,3*]
[1] *Department of Physics, School of Biomedical Engineering, Third Military Medical University, Chongqing 400038, China.*
[2] *Institute of High Energy Physics, Chinese Academy Sciences, P.O. Box 918(4), Beijing, 100049, China.*
[3] *Theoretical Physics Center for Science Facilities, CAS, Beijing, 100049, China.*
(Dated: March 25, 2014)

In this paper, we present the study of the hadroproduction rate of h_c at next-to-leading order in α_s under the nonrelativisitic QCD (NRQCD) factorization framework, using long-distance matrix elements obtained from the fit of χ_c production measurements by LHCb. We consider the problem of NRQCD scale dependence for the first time, and find that, for some experimental conditions, the choice of this scale can substantially affect the final results. Up to this order, color-octet channel still contribute the most part of the production rate.

PACS numbers: 12.38.Bx, 12.39.St, 13.85.Ni, 14.40.Pq

arXiv:1403.5944v1 [hep-ph] 24 Mar 2014

In the last ten years, many experimental measurements for P-wave quarkonia $h_c, h_b(1^{+-})$ have been achieved. The related branching ratios [1–6], the masses of these quarkonia [7–11], as well as the cross sections for $h_c(h_b)$ production via e^+e^- annihilation at the CLEO-c [10] and B-factories [11] are measured. In contrast, only leading order (LO) results have been given for h_c (h_b) productions. The calculations of h_c hadroproduction at the Tevatron [12] and LHC [13, 14] predicted a significant yield. Photoproduction of h_c was investigated in Ref. [15] by using a color-octet (CO) long-distance matrix element (LDME) extracted from the decay $B \to \chi_{cJ} + X$; the results indicated a significant cross section at the DESY HERA. h_c production through e^+e^- annihilation was investigated in two recent papers [16, 17], the former of which included the results for h_b as well. Since next-to-leading order (NLO) corrections noticeably change the behavior of the transverse momentum (p_t) distribution of the production rate of P-wave quarkonia through color-singlet (CS) channel, in order to investigate h_c production in nonrelativistic QCD (NRQCD) [18] framework, calculation up to this order is required.

However, no adequate experimental data has come out to extract the CO LDME for h_c production directly. Thanks to the spin symmetry at LO of NRQCD expansion, we can simply estimate this LDME as that of ${}^3S_1^{[8]}$ state for χ_{c1} production, of which both LO and NLO values have already been given in sevaral papers [19–22]; the first three employed experimental data of CDF [23] while the last one added the LHCb data [24] to carry out a global fit.

In this paper, we study h_c production at hadron colliders at NLO of QCD coupling constant α_s. New fitted CO LDMEs will be given for different values of NRQCD scale. Employing these LDMEs, we present numerical results for Tevatron and LHC energy.

In NRQCD framework, at LO of v (the relative velocity of quark and antiquark in quarkonium), differential cross sections for h_c hadroproduction can be expressed as

$$\begin{aligned} d\sigma(pp \to h_c + X) &= df(pp \to (c\bar{c})_n + X)\langle O_n^{h_c}\rangle \\ &= \sum_{i,j,n} \int dx_1 dx_2 G(x_1, i) G(x_2, j) d\hat{f}(i + j \to (c\bar{c})_n + X)\langle O_n^{h_c}\rangle, \end{aligned} \tag{1}$$

where p denotes either a proton or an antiproton, the indices i, j run over all partonic species, n denotes a definite $c\bar{c}$ state of certain color and angular momentum, $G(x, i)$ is the parton-distribution-function (PDF) with x being the ratio of the momentum of parton i to that of the proton or antiproton, $\hat{f}$ represents the parton-level short-distance coefficient, which can be evaluated perturbatively in α_s and v. Since our calculation is up to LO in v, only two channels ${}^1P_1^{[1]}$ and ${}^1S_0^{[8]}$ are involved.

The LO partonic processes are listed as

$$g + g \to c\bar{c}({}^1P_1^{[1]}) + g, \tag{2}$$

*Electronic address: hfzhang@ihep.ac.cn

and

$$\begin{aligned} g+g &\to c\bar{c}(^1S_0^{[8]})+g, \\ g+q &\to c\bar{c}(^1S_0^{[8]})+q, \\ q+\bar{q} &\to c\bar{c}(^1S_0^{[8]})+g. \end{aligned} \tag{3}$$

The procese in Eq.(2) generates $^1P_1^{[1]}$ state, while the three processes in Eq.(3) generate $^1S_0^{[8]}$ state. Both of the two states transit into h_c through long-distance processes which can not be evaluated perturbatively, and the transition rates are described by LDMEs. The LDME of $^1P_1^{[1]}$ can be expressed in terms of radial derivative of the wave function of quarkonium at the origin:

$$\langle O^{h_c}_{^1P_1^{[1]}}\rangle = \frac{27}{2\pi}|R'_{h_c}(0)|^2, \tag{4}$$

while that of $^1S_0^{[8]}$ is obtained from the fit of experimental measurements of χ_c productions. To evaluate the short-distance coefficients, we notice they are independent of the long-distance asymptotic states, and replace h_c in Eq.(1) by an on-shell heavy quark pair state with definite quantum numbers, the following equations can be obtained,

$$d\sigma_m = \sum_n df_n \langle O_n^m\rangle, \tag{5}$$

where, and through out the rest of this paper, we denote the cross sections $\sigma(pp \to n+X)$ and short-distance coefficients $f(pp\to n+X)$ in abbreviation as σ_n and f_n, respectively. The cross section for producing m can be evaluated perturbatively in α_s by reading the amplitudes from Feynman diagrams. For $^1P_1^{[1]}$ state, up to leading order in v, only two states, $^1P_1^{[1]}$ and $^1S_0^{[8]}$, are involved, thus, we have

$$d\sigma_{^1P_1^{[1]}} = df_{^1P_1^{[1]}}\langle O^{^1P_1^{[1]}}_{^1P_1^{[1]}}\rangle + df_{^1S_0^{[8]}}\langle O^{^1P_1^{[1]}}_{^1S_0^{[8]}}\rangle. \tag{6}$$

At LO in α_s, $\langle O_n^m\rangle$ vanishes unless $m=n$, as a result, the short-distance coefficients can be simply expressed in terms of integrated squared amplitudes.

Up to NLO in α_s, the calculation of $^1S_0^{[8]}$ state production has been described in detail in our previous paper [25]. Here we focus on $^1P_1^{[1]}$ state production at this order. The processes involved are as follows,

$$\begin{aligned} V: g+g &\to c\bar{c}(^1P_1^{[1]})+g, \\ g+g &\to c\bar{c}(^1P_1^{[1]})+gg, \\ g+g &\to c\bar{c}(^1P_1^{[1]})+q\bar{q}, \\ g+q &\to c\bar{c}(^1P_1^{[1]})+gq, \\ q+\bar{q} &\to c\bar{c}(^1P_1^{[1]})+gg. \end{aligned} \tag{7}$$

where lable V means one-loop virtual corrections for the process on the right side of it. Summing all the processes, one finds the IR divergences do not cancel, which can be figured out in NRQCD framework by subtracting the divergence coming out of $\langle O^{^1P_1^{[1]}}_{^1S_0^{[8]}}\rangle$. Up to the order maintained in our calculation, the transition rate of $c\bar{c}$ state $^1S_0^{[8]}$ into $^1P_1^{[1]}$ can be calculated in dimensional regularization and $\overline{MS}$ renormalization scheme as

$$\langle O^{^1P_1^{[1]}}_{^1S_0^{[8]}}\rangle^{NLO} = -\frac{\alpha_s}{3\pi m_c^2}u_\epsilon^c \frac{N_c^2-1}{N_c^2}\langle O^{^1P_1^{[1]}}_{^1P_1^{[1]}}\rangle^{LO}, \tag{8}$$

where N_c is 3 for $SU(3)$ gauge field and u_ϵ^c is defined as

$$u_\epsilon^c = \frac{1}{\epsilon_{IR}} - \gamma_E - \frac{1}{3} + ln(\frac{4\pi\mu_R^2}{\mu_\Lambda^2}), \tag{9}$$

with γ_E being Euler's constant. The divergence in this LDME will cancel that in $\sigma(^1P_1^{[1]})$, which can be isolated by using the two-cutoff phase space slicing method [26] as

$$\begin{aligned} d\sigma_{^1P_1^{[1]}} &= d\sigma^{L+V}_{^1P_1^{[1]}} + d\sigma^{S}_{^1P_1^{[1]}} + d\sigma^{H}_{^1P_1^{[1]}} \\ &= (df^{L+V+S_1}_{^1P_1^{[1]}} + df^{H}_{^1P_1^{[1]}} + df^{S_2}_{^1P_1^{[1]}})\langle O^{^1P_1^{[1]}}_{^1P_1^{[1]}}\rangle, \end{aligned} \tag{10}$$

where σ^{L+V} represents the summation of LO and virtual correction contributions, and σ^S and σ^H are real corrections from the gluon-soft and -hard region, respectively. The boundary of the two regions is $E_g = \frac{\sqrt{s}}{2}\delta_s$, where E_g is the energy of the soft gluon and δ_s is an arbitrary positive number small enough to provide the soft approximation with adequate accuracy. Moreover, the gluon-soft region consists of where the soft gluon is attached to an external charm quark (antiquark) line (labeled S_2) and where it is attached to other external lines (labeled S_1). Noticing that we have summed over all the processes in Eq.(7), the only divergent term left in $d\sigma_{^1P_1^{[1]}}$ comes from $df^{S_2}_{^1P_1^{[1]}}$ which will subtract the divergence in $\langle O^{^1P_1^{[1]}}_{^1S_0^{[8]}}\rangle$. Neglecting the finite terms in this small region, the soft part can be expressed as

$$d\sigma^{S_2}_{^1P_1^{[1]}} = -\frac{\alpha_s}{3\pi m_c^2} u_\epsilon^s \frac{N_c^2-1}{N_c^2} df_{^1S_0^{[8]}} \langle O^{^1P_1^{[1]}}_{^1P_1^{[1]}}\rangle, \tag{11}$$

where

$$u_\epsilon^s = \frac{1}{\epsilon_{IR}} + \frac{E}{p} ln(\frac{E+p}{E-p}) + ln(\frac{4\pi\mu_R^2}{s\delta_s^2}) - \gamma_E - \frac{1}{3}, \tag{12}$$

where E and p are energy and absolute value of momentum of h_c.

Matching Eq.(6) and Eq.(10), at the same time, employing Eq.(8) and Eq.(11), and constrain our calculation up to NLO in α_s, we obtain the expression of short-distance coefficient for $^1P_1^{[1]}$ state as

$$df^{NLO}_{^1P_1^{[1]}} = df^{L+V+S_1}_{^1P_1^{[1]}} + df^{H}_{^1P_1^{[1]}} - \frac{\alpha_s}{3\pi m_c^2}\frac{N_c^2-1}{N_c^2} u_\epsilon df^{LO}_{^1S_0^{[8]}}, \tag{13}$$

where

$$u_\epsilon = u_\epsilon^s - u_\epsilon^c = \frac{E}{p} ln(\frac{E+p}{E-p}) + ln(\frac{\mu_\Lambda^2}{s\delta_s^2}). \tag{14}$$

It is clearly shown that all the short-distance coefficients are IR divergence free and the cross section for the first process is well defined. To calculate $\sigma(^1S_0^{[8]})$ and $\sigma^S(^1P_1^{[1]})$, we apply our Feynman Diagram Calculation package (FDC) [27] to generate all the needed FORTRAN source.

From the heavy quark spin symmetry of the NRQCD Lagrangian, it is obvious that the LDME $\langle O^{h_c}_{^1S_0^{[8]}}\rangle$ for the intermediate state $c\bar{c}(^1S_0^{[8]})$ evolving into h_c is exactly the same as that for the intermediate state $c\bar{c}(^3S_1^{[8]})$ evolving into χ_c at LO of v^2. It gives

$$\langle O^{h_c}_{^1S_0^{[8]}}\rangle \approx \langle O^{\chi_{c1}}_{^3S_1^{[8]}}\rangle. \tag{15}$$

Substituting Eq.(13) into Eq.(1), we obtain the complete expression of cross section for h_c production,

$$d\sigma^{NLO}_{h_c} = \langle O^{h_c}_{^1P_1^{[1]}}\rangle (df^{L+V+S_1}_{^1P_1^{[1]}} + df^{H}_{^1P_1^{[1]}}) - \frac{\alpha_s}{3\pi m_c^2}\frac{N_c^2-1}{N_c^2} u_\epsilon \langle O^{h_c}_{^1P_1^{[1]}}\rangle df^{LO}_{^1S_0^{[8]}} + \langle O^{h_c}_{^1S_0^{[8]}}\rangle df^{NLO}_{^1S_0^{[8]}}. \tag{16}$$

If we proceed our calculation to infinite order of α_s, the μ_Λ dependence can be totally absorbed into the CO LDME. As a result, this scale actually can be any positive value holding the convergence of α_s expansion. If our results dramatically depend on μ_Λ, the dropped terms in higher orders must contribute significantly, and the calculation up to this order does not reach a sufficient accuracy. Up to NLO, the condition of μ_Λ independence requires

$$\frac{\alpha_s}{3\pi m_c^2}\frac{N_c^2-1}{N_c^2} df^{LO}_{^1S_0^{[8]}} \propto df^{NLO}_{^1S_0^{[8]}}, \tag{17}$$

as well as that the proportional ratio be universal for all the processes. Actually, in most of the cases, this condition can not be satisfied.

To show the problem of μ_Λ dependence, at the same time, to determine whether α_s expansion up to this order have got an adequate accuracy, one should carry out the calculation at different values of this scale. The fitting should also be carried out at each perticular scale.

In the numerical calculation, we have the following common choices as $|R'_{h_c}(0)|^2 = 0.075$ GeV^5 [28] for both LO and NLO calculation, $\langle O^{h_c}_{^1S_0^{[8]}}\rangle_{LO} = 0.0098$ GeV^3, the same as Ref. [20], and $m_c = 1.5$ GeV. The soft cutoff δ_s

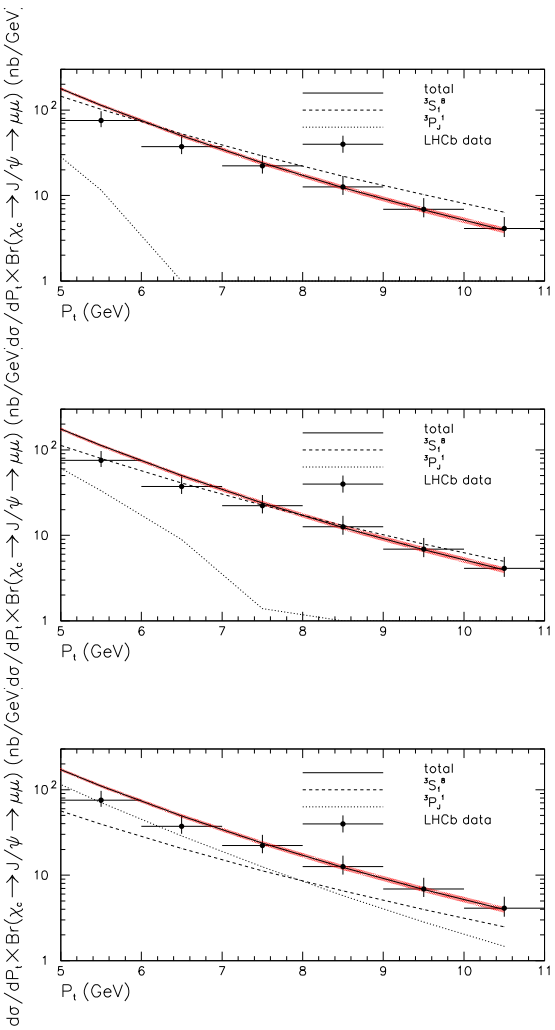

FIG. 1: Fit of the LHCb [24] data with the branching ratio of χ_c to J/ψ multiplied. The values of μ_Λ are m_c, $m_c/2$ and Λ_{QCD} for upper, middle and lower figures, respectively.

independence is checked in the calculation and $\delta_s = 0.001$ is used. Since the energy scale of most of the phase space region exceeds b-quark mass, $\Lambda_{QCD}|_{nf=5} = 0.226$ GeV is used. We employ CTEQ6M [29] as PDF and two-loop α_s running for NLO calculation, and CTEQ6L1 [29] and one-loop α_s running for LO.

We employ LHCb [24] data for χ_c production, excluding $p_t < 7$ GeV points, to obtain the value of the CO LDME. The CM energy and rapidity cut are $\sqrt{s} = 7000$ GeV and $2 < y < 4.5$, respectively. The CO LDMEs are obtained as

$$\begin{aligned}
\langle O^{h_c}_{^1S_0^{[8]}} \rangle_{m_c} &= (0.73 \pm 0.01) \times 10^{-2}\ \text{GeV}^3 \\
\langle O^{h_c}_{^1S_0^{[8]}} \rangle_{m_c/2} &= (0.57 \pm 0.01) \times 10^{-2}\ \text{GeV}^3 \\
\langle O^{h_c}_{^1S_0^{[8]}} \rangle_{\Lambda_{QCD}} &= (0.28 \pm 0.01) \times 10^{-2}\ \text{GeV}^3
\end{aligned} \tag{18}$$

where the values of μ_Λ are labeled at the foot of LDMEs.

Fig. 1 shows p_t distributions of the production rates for χ_c generated J/ψ, from which we can see that, for all the three values of the scale, our calculations can fit the experimental data well. Employing these LDMEs, h_c production rate for three experimental conditions are presented in the following.

For Tevatron energy, i.e. $\sqrt{s} = 1.96$TeV, and rapidity cut condition $|y| < 0.6$, denoted as experimental condition I, h_c production rates are presented in Fig. 2. As is shown in these figures, $^1S_0^{[8]}$ channel contribute most of the positive part of the total production, just as the situation for LO. Despite the contributions from the two channels, $^1S_0^{[8]}$ and $^1P_1^{[1]}$, vary significantly for different choices of the NRQCD scale, the final results are not affected noticeably. The

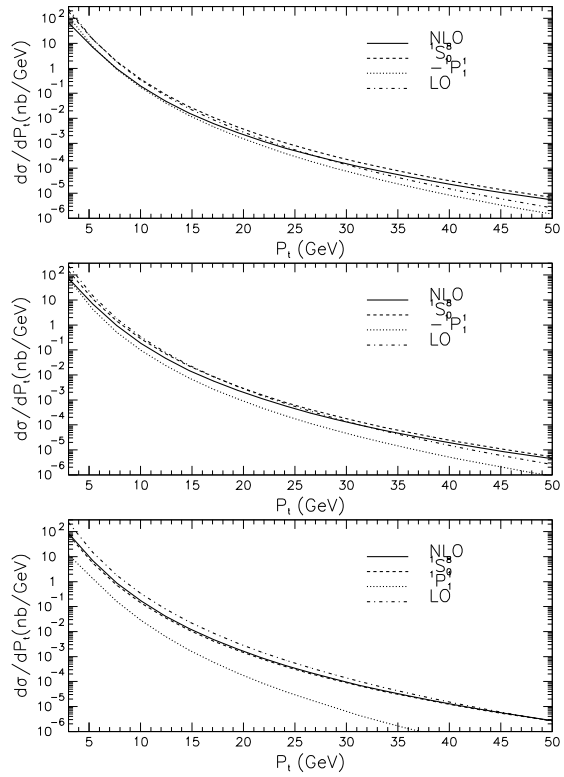

FIG. 2: h_c producton at the Tevatron. The CM energy and rapidity cut are $\sqrt{s} = 1960$ GeV and $|y| < 0.6$, respectively. The values of μ_Λ are m_c, $m_c/2$ and Λ_{QCD} for upper, middle and lower figures, respectively.

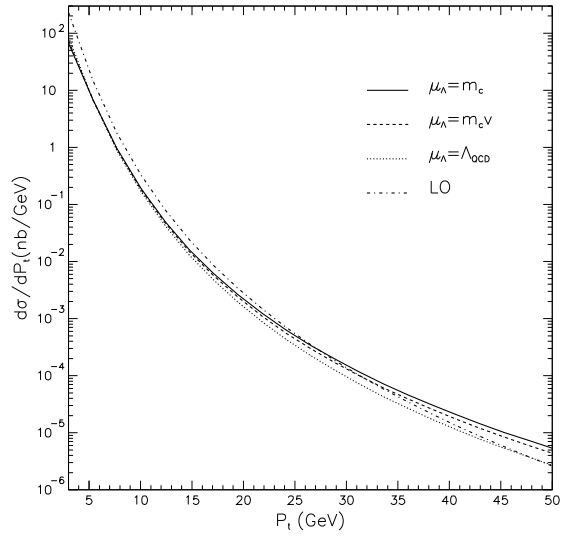

FIG. 3: The comparison of the results for the three different choices of NRQCD scale. The CM energy and rapidity cut are $\sqrt{s} = 1960$ GeV and $|y| < 0.6$, respectively.

distinction of the final results for the three scale choices is presented more explicitly in Fig. 3. We can see that, in low p_t region, different values of this scale bring in little distinction, while in high p_t region, the three curves differ, but not much (the largest is about twice the amplitude of the smallest). Since large logarithm term $ln(m_c/p_t)$ may ruin α_s expansion for both too large and too small p_t, besides, in small p_t region, relativisitic corrections contribute a nonlinear remarkable part, only medium p_t region is considered up to this order in this paper. Restricted to this region, our results do not depend on NRQCD scale significantly. We can say the dependence of this scale has been absorbed into the CO LDME, which turns out to be a scale-relevant quantity.

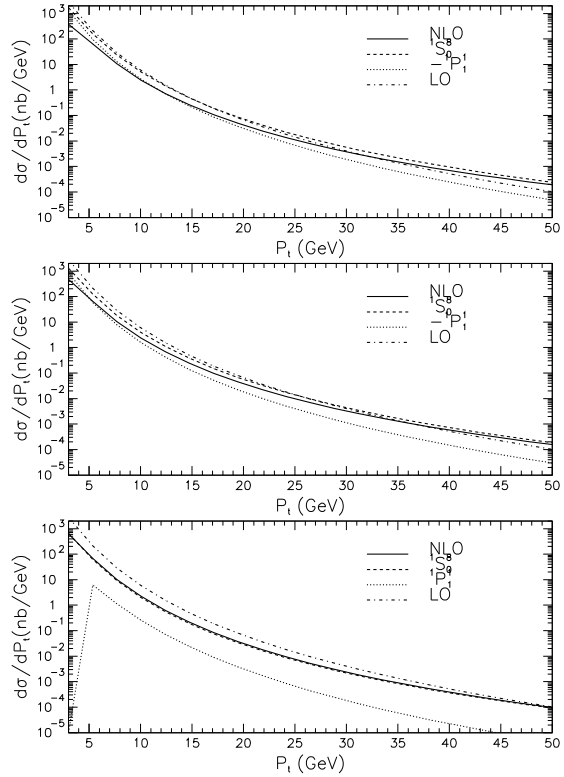

FIG. 4: h_c producton at the LHC. The CM energy and rapidity cut are $\sqrt{s} = 7000$ GeV and $|y| < 2.4$, respectively. The values of μ_Λ are m_c, $m_c/2$ and Λ_{QCD} for upper, middle and lower figures, respectively.

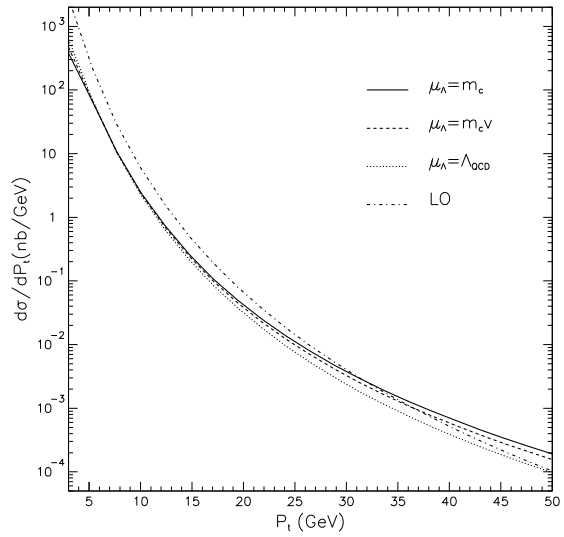

FIG. 5: The comparison of the results for the three different choices of NRQCD scale. The CM energy and rapidity cut are $\sqrt{s} = 7000$ GeV and $|y| < 2.4$, respectively.

For LHC energy $\sqrt{s} = 7$TeV, while rapidity range being $|y| < 2.4$, denoted as experimental condition II, we got similar conclusion; NRQCD scale dependence is not severe to ruin the accuracy of prediction, as is shown in Fig. 4 and Fig. 5.

However, at the same LHC energy, for $2.5 < y < 4.0$, denoted as experimental condition III, when $\mu_\Lambda = m_c$ and $m_c/2$, we got unphysical results, i.e. negative cross sections. The dependence of NRQCD scale is so dramatic that we cannot make a definite conclusion for this experimental condition. Only for $\mu_\Lambda = \Lambda_{QCD}$, the cross section turns out to be positive through out the whole range of p_t. The comparison of the results for the three different choices

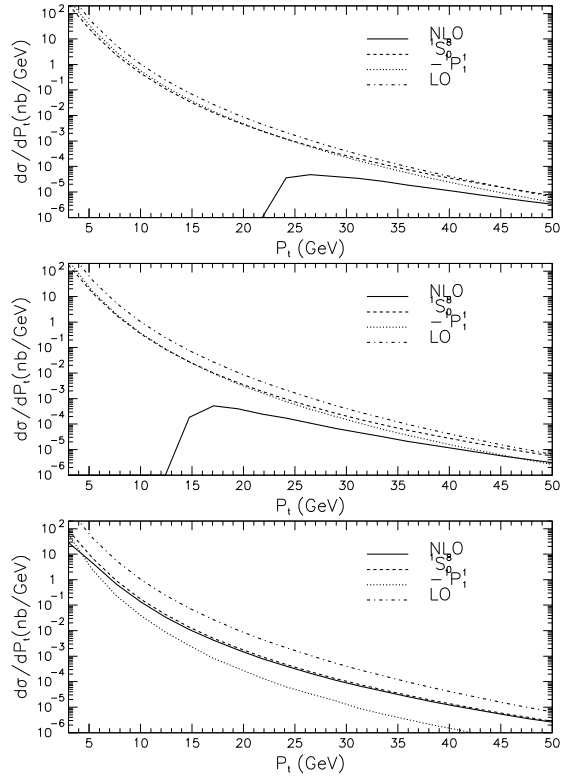

FIG. 6: h_c producton at the LHC. The CM energy and rapidity cut are $\sqrt{s} = 7000$ GeV and $2.5 < y < 4$, respectively. The values of μ_Λ are m_c, $m_c/2$ and Λ_{QCD} for upper, middle and lower figures, respectively.

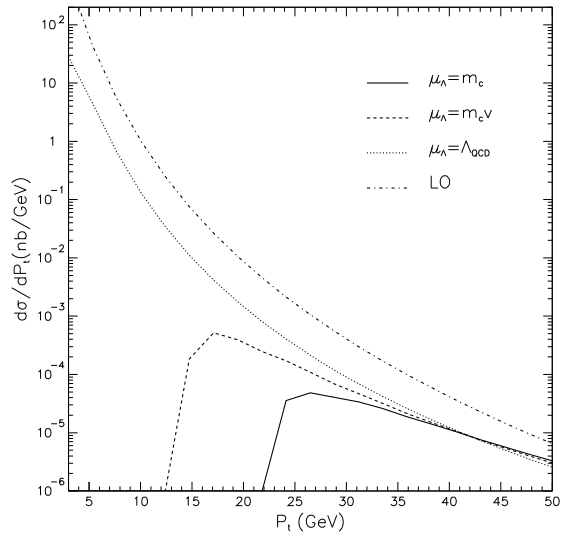

FIG. 7: The comparison of the results for the three different choices of NRQCD scale. The CM energy and rapidity cut are $\sqrt{s} = 7000$ GeV and $2.5 < y < 4$, respectively.

of NRQCD scale is also presented, as is shown in Fig. 7. We notice that, for a proper determined NRQCD scale m_c, i.e. it is comparable to other scales in this calculation and in perturbative region, even for medium p_t, where no resummation is required, we come across unphysical results. This indicates that higher order corrections must be sizeable, and up to this order, the results are not reliable.

In order to investigate the origin of this discrepency of the three curves for the third experimental condition, we

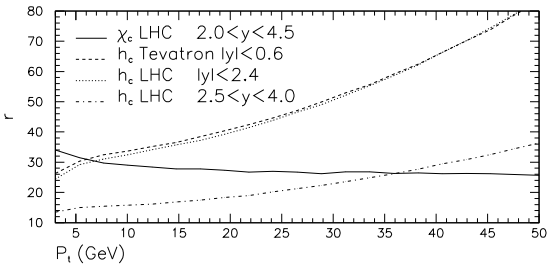

FIG. 8: The comparison of the value of r for the three different experimental conditions for h_c, as well as χ_c, as a function of p_t. The CM energy for LHC and Tevatron experiment are $\sqrt{s} = 7000$ GeV and $\sqrt{s} = 1960$ GeV, respectively.

define the proportional ratio for Eq.(17) as

$$r = \frac{df_n^{NLO}}{dp_t}/(\frac{\alpha_s}{3\pi}\frac{N_c^2-1}{N_c^2}\frac{df_n^{LO}}{dp_t}), \tag{19}$$

where n is either ${}^1S_0^{[8]}$ or ${}^3S_1^{[8]}$. We calculate this parameter for h_c productions for the three experimental conditions, as well as that for χ_c production for the experimental condition we used in the fit. Fig. 8 compares the values of r for the four conditions. In the case of χ_c production, the dependence of r on p_t is flat, which explains the fact that, the experiment can be fitted well for all the three choices of the scale. At small and medium p_t, the curve for χ_c is close to that for h_c in condition I and II. This results in slight μ_Λ dependence in the two conditions, just as shown in Fig. 3 and 5. However, for condition III, the value of r is quite (about two and a half time) below that for χ_c, which causes the scale dependence problem, as is shown in Fig. 7. In high p_t region, the curves for condition I and II are quite above that for χ_c, the corresponding effect is that, in this p_t region, the dependence of the production rates of h_c on NRQCD scale is more remarkable than in low p_t region. By contrast, this problem for condition III becomes milder in this p_t region.

In summary, we present the QCD NLO theoretical predictions of the h_c production at the Tevatron and the LHC. At this order, CO channel counts for most of the positive contributions to the production rate of h_c, while the CS channel contributes a small positive or negative part. LO curves are above NLO ones in low p_t region for all the three conditions. For experimental conditions I and II, LO and NLO curves get close to and intersect with each other as p_t increases. Using the CO LDMEs for different values of NRQCD scale, we study the NRQCD scale (μ_Λ) dependence of h_c hadroproduction rate. In medium p_t region, where perturbative calculation is available, for the first two conditions, the final results depend on μ_Λ slightly, as a result, theoretical predictions up to this order are reliable. The production rates are physical for all the choices of μ_Λ considered in this paper for these two conditions, in contrast to a negative production rate in low (and medium) p_t range for condition III while setting μ_Λ as m_c (and $m_c/2$). In the third condition, the theoretical prediction remarkably depend on μ_Λ in medium p_t range, as a result, theoretical prediction for this experimental condition fails at this order. Our calculations for LO results agree with Ref. [14] when employing the same choices of parameters, yet cannot accord with Ref. [12, 13] despite having tried all the possible choices of parameters.

This work is supported by the National Natural Science Foundation of China (Nos. 10979056 and 10935012), in part by DFG and NSFC (CRC 110) and CAS under Project No. INFO-115-B01.

[1] G. Calderini (BaBar Collaboration), pp. 71–76 (2004), hep-ex/0405081.
[2] M. Andreotti, S. Bagnasco, W. Baldini, D. Bettoni, G. Borreani, et al., Phys.Rev. **D72**, 032001 (2005).
[3] F. Fang et al. (Belle Collaboration), Phys.Rev. **D74**, 012007 (2006), hep-ex/0605007.
[4] M. Ablikim et al. (BESIII Collaboration), Phys.Rev.Lett. **104**, 132002 (2010), 1002.0501.
[5] J. Lees et al. (BABAR Collaboration), Phys.Rev. **D84**, 091101 (2011), 1102.4565.
[6] J. Ge et al. (CLEO Collaboration), Phys.Rev. **D84**, 032008 (2011), 1106.3558.
[7] J. Rosner et al. (CLEO Collaboration), Phys.Rev.Lett. **95**, 102003 (2005), hep-ex/0505073.
[8] P. Rubin et al. (CLEO Collaboration), Phys.Rev. **D72**, 092004 (2005), hep-ex/0508037.
[9] S. Dobbs et al. (CLEO Collaboration), Phys.Rev.Lett. **101**, 182003 (2008), 0805.4599.
[10] T. Pedlar et al. (CLEO Collaboration), Phys.Rev.Lett. **107**, 041803 (2011), 1104.2025.
[11] I. Adachi et al. (Belle Collaboration), Phys.Rev.Lett. **108**, 032001 (2012), 1103.3419.
[12] K. Sridhar, Phys.Rev.Lett. **77**, 4880 (1996), hep-ph/9609285.

[13] K. Sridhar, Phys.Lett. **B674**, 36 (2009), 0812.0474.
[14] C.-F. Qiao, D.-L. Ren, and P. Sun, Phys.Lett. **B680**, 159 (2009), 0904.0726.
[15] S. Fleming and T. Mehen, Phys.Rev. **D58**, 037503 (1998), hep-ph/9801328.
[16] J.-X. Wang and H.-F. Zhang, Phys.Rev. **D86**, 074012 (2012), 1207.2416.
[17] Y. Jia, W.-L. Sang, and J. Xu (2012), 1206.5785.
[18] G. T. Bodwin, E. Braaten, and G. P. Lepage, Phys.Rev. **D51**, 1125 (1995), hep-ph/9407339.
[19] P. L. Cho and A. K. Leibovich, Phys.Rev. **D53**, 150 (1996), hep-ph/9505329.
[20] P. L. Cho and A. K. Leibovich, Phys.Rev. **D53**, 6203 (1996), hep-ph/9511315.
[21] Y.-Q. Ma, K. Wang, and K.-T. Chao, Phys.Rev. **D83**, 111503 (2011), 1002.3987.
[22] B. Gong, L.-P. Wan, J.-X. Wang, and H.-F. Zhang (2012), 1205.6682.
[23] F. Abe et al. (CDF Collaboration), Phys.Rev.Lett. **79**, 578 (1997).
[24] R. Aaij et al. (LHCb Collaboration) (2012), 1204.1462.
[25] B. Gong, X. Q. Li, and J.-X. Wang, Phys.Lett. **B673**, 197 (2009), 0805.4751.
[26] B. Harris and J. Owens, Phys.Rev. **D65**, 094032 (2002), hep-ph/0102128.
[27] J.-X. Wang, Nucl.Instrum.Meth. **A534**, 241 (2004), hep-ph/0407058.
[28] E. J. Eichten and C. Quigg, Phys.Rev. **D52**, 1726 (1995), hep-ph/9503356.
[29] J. Pumplin, D. Stump, J. Huston, H. Lai, P. M. Nadolsky, et al., JHEP **0207**, 012 (2002), hep-ph/0201195.